DALTON
FULL PAPER

Organic–inorganic hybrid solids: control of perhalometallate solid state structures †

Amy L. Gillon,[a] Gareth R. Lewis,[a] A. Guy Orpen,*[a] Sarah Rotter,[a] Jonathan Starbuck,[a] Xi-Meng Wang,[a] Yolanda Rodríguez-Martín[b] and Catalina Ruiz-Pérez[b]

[a] *School of Chemistry, University of Bristol, Bristol, UK BS8 1TS*
[b] *Departemento de Física Fundamental II, Universidad de La Laguna, 38204 La Laguna, Spain*

Received 23rd June 2000, Accepted 27th July 2000
First published as an Advance Article on the web 25th September 2000

MX···HN$^+$ hydrogen bond synthons have been exploited in preparation of crystalline salts [4,4′-H$_2$bipy][MX$_4$] [X = Cl, M = Pd, Pt, Co, Zn, Hg, Mn, Cd and Pb; X = Br, M = Pd, Co, Zn and Mn]. In these salts three structural forms for the halometallate species are observed: mononuclear square planar (M = Pd, Pt) or tetrahedral (M = Co, Zn, Hg) and polymeric *cis* edge-sharing octahedral (M = Mn, Cd, Pb). These correspond to three structural motifs which form the basis of the crystal structures formed in their [4,4′-H$_2$bipy]$^{2+}$ salts: ribbon polymer (M = Pt, Pd); herring-bone packing of cyclic dimers (M = Co, Zn, Hg); layer cross-linked polymers [{MX$_4$}$_n$]$^{2n-}$ (M = Mn, Cd, Pb). The factors controlling the structures adopted, the hierarchy of intermolecular interactions present in these crystals and the principles that may be inferred and exploited further are considered.

Introduction

Long-term aims in the field of crystal engineering amount to the development of a new chemistry of the solid state—where control over the architecture, metrics, dimensionality and properties of synthetic crystalline solids is as sophisticated as is currently possible in molecular synthesis. This would shift the focus of the crystallography of molecular solids from the 20th century mode in which it has been dominated by *analysis* (the determination of crystal structures and the analysis of the information they contain), to the *synthesis* of new crystalline phases, using the principles established from these analyses. There is currently great interest in this sort of crystal engineering and related supramolecular and materials chemistry and the application of hydrogen bonding to control molecular aggregation, as witnessed by the papers cited in refs. 1 and 2. In this paper we draw the attention of scientists in these fields to experimental evidence for the synthetic utility of the hydrogen bonding properties of metal halides in the synthesis of novel crystal structures.

The synthetic aspects of crystal engineering (*i.e.* crystal structure synthesis) to date have been dominated by organic solid state chemistry (as exemplified by the work of Desiraju)[1] and coordination polymer chemistry (*e.g.* the work of Robson, Iwamoto, Schröder and others)[3] in which the hydrogen bond and the dative coordinate bond respectively have afforded the required links between molecular units. The potential for metals to control the aggregation of molecular species through hydrogen bonding and at the same time to provide potentially useful properties has received much less attention.[4]

The strategies that have been adopted in the field of crystal structure synthesis may be divided into two main camps: (i) those that seek to exploit the shape-controlled close packing of molecules and (ii) those that exploit specific (local) interactions to control aggregation of molecular species. In exploring strategy (i) we have studied the possibility of computing alternative viable crystal structures of relatively rigid metal complexes with weakly directional intermolecular interactions. In the case of the archetypal organometallic complexes [M(CO)$_n$] ($n = 4$, M= Ni; $n = 5$, M = Fe; $n = 6$, M = Cr),[5] we were able to show that while it is possible to reproduce their crystal structures well given a good starting point, it is not yet possible to generate the crystal structures reliably *ab initio* given only a good estimate of the molecular geometry. In parallel experimental work we prepared a series of novel low dimensional salts of planar platinum- and palladium-containing anions with structure-dependent magnetic characteristics.[6] In that work redox-active organometallic building blocks of well defined shape were used to synthesise crystals in which the magnetic properties of the component ions and the stoichiometry and structures of the solids were varied systematically in order to explore the relationship between crystal structure and magnetic behaviour. We have explored a shape-based strategy in the preparation of heteromolecular solids containing planar diborane(4) species and electron acceptor species such as tetracyanoethylene (tcne) and tetracyanoquinodimethane (tcnq).[7] We have used the CSD to understand the directionality of secondary (in Alcock's terminology) hypervalent bonding of the heavy p-block elements, in order to highlight its potential to mimic hydrogen bonding in controlling aggregation of molecular species in crystals.[8] Subsequently we have been able to show that such interactions do indeed afford crystal structures of partly predictable form.[9]

Here, we follow strategy (ii) in which Desiraju has suggested that success lies in the identification of "supramolecular synthons" that may be relied upon to form between molecules with the appropriate functional groups and thereby control their aggregation, drawing an analogy with the synthon concept in organic synthetic chemistry which facilitates the design of molecules through reliably formed connections between functional groups.

In the quest for methods that can be reliably exploited in the preparation of new solids by design, robust synthons are necessary but they may not be sufficient. A higher level of control, over not just local structure but over periodic structure at the unit cell scale, is required, at what we shall call the motif level.

---

† Based on the presentation given at Dalton Discussion No. 3, 9–11th September 2000, University of Bologna, Italy.

Electronic supplementary information (ESI) available: rotatable 3-D crystal structure diagram in CHIME format. See http://www.rsc.org/suppdata/dt/b0/b005036i/

DOI: 10.1039/b005036i

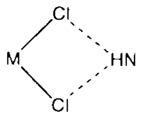

A

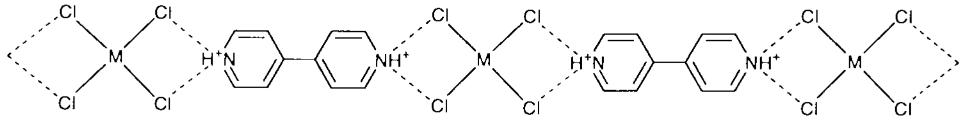

B

Such reliable structural motifs should incorporate molecular building blocks (having covalent frameworks) or even supramolecular building blocks (having partly non-covalent frameworks) and be linked by robust supramolecular synthons. The motifs formed are then cross-linked by other intermolecular interactions of varying strength to form the full crystal structure. This paper is set within this conceptual framework. Complex ions with hydrogen bonding capability are used as building blocks to prepare crystal structures in which the metrics of the structure, the dimensionality of the networks and the physical properties of the solid can be brought under a degree of chemical control.

In classical inorganic solid state chemistry the focus is on "atomic" ions (typically metal cations and oxide or fluoride anions) whose electrostatic (Madelung) lattice energies promote formation of highly stable extended array structures. In organic molecular solid state chemistry the emphasis has been on hydrogen bonded or close-packed structures with lower lattice energies derived from hydrogen bonding and dispersive, van der Waals, interactions. In this paper elements from both these fields are at work and the focus is on using both inorganic and organic components to form new crystalline solids that fall within Mitzi's definition of organic–inorganic hybrid composites.[10] We use hydrogen bonding to control the relative local arrangements of the anions and cations in the solid salts while raising the lattice energy (and the hydrogen bond contribution to it) through the use of ionic building blocks. The consequent melting point, mechanical and solubility properties of the salts are likely to contrast with those of their neutral "organic" counterparts and may play a role in their potential applications.

The ability to incorporate metal ions into a designed crystal structure offers promise of novel functionalities (chemical, magnetic, optical or electronic) which complement those available in purely organic molecular crystals. Preparation of coordination polymers provides one route to this end, widely explored in recent times.[3] Others have exploited the possibility of using organic ligands with hydrogen bonding capability (some including multiple complementary sites such as nuclear base derivatives) as a means to crystal structure synthesis of metal complexes.[11] In this work we emphasise the possibility of exploiting the ability of the metal both to facilitate hydrogen bonding by affecting the ability of its attached ligands to act as hydrogen bond acceptors and to provide a framework on which to hang the hydrogen bonds.

Using the Cambridge Structural database (CSD) we have explored the nature of intermolecular interactions that involve metal complexes, and have reported that in the case of transition metal chloride complexes, M–Cl moieties are much better hydrogen bond acceptors than are their organic analogues (organochlorine species, C–Cl).[12] Here, we report that the hydrogen bonding capability of the $[4,4'\text{-H}_2\text{bipy}]^+$ dication allows preparation of three classes of $[4,4'\text{-H}_2\text{bipy}][\text{MX}_4]$ (X = Cl, Br) structures based on square planar or tetrahedral and polymerised $[\text{MCl}_4]^{2-}$ entities. Some of these results have been communicated in preliminary form.[13,14]

Results

The ability of metal chloride complexes to act as hydrogen bond acceptors has been noted both in our database work and previously in specific examples (see for example, refs. 15). These metal-assisted hydrogen bonds typically have short MCl···HN (or HO) distances in the range 2.2–2.6 Å and M–Cl···H angles in the range 90–120° with normal angles at hydrogen[16] (*e.g.* N–H···Cl ≥ *ca.* 140°). This set of characteristics is consistent with the stability of hydrogen bond interactions of form **A** as observed in $[\text{HNC}_5\text{H}_3\text{Ph}_2][\text{AuCl}_4]$.[15a] We set out to test the *cis*-MCl_2···HN interaction (**A**) as a synthon for the preparation of a hydrogen bonded ribbon motif (**B**) containing complex ions of inorganic ($[\text{MCl}_4]^{2-}$) and organic ($[4,4'\text{-H}_2\text{bipy}]^{2+}$) character. Reaction of aqueous $[\text{MCl}_4]^{2-}$ salts (M = Pd or Pt) with $[4,4'\text{-H}_2\text{bipy}]^{2+}$ gives crystalline precipitates $[4,4'\text{-H}_2\text{bipy}][\text{MCl}_4]$ [M = Pd (**1**), Pt (**2**)]. Single crystal structure analysis of a sample of **2** prepared with improved, slower crystallisation techniques compared with that first reported,[13] shows the desired structure has indeed been formed (see Table 1, Figs. 1 and 2). Powder diffraction data for **1** indicate that it is isostructural with **2**. The component ions in **2** have normal, planar geometries. The N–H···Cl bonds are of geometries consistent with expectations based on our database study[12] (N–H 1.02 Å, H···Cl 2.40 Å, N···Cl 3.216 Å; N–H···Cl 136°, Pt–Cl···H 92.4°). The ribbons formed are planar (mean atomic deviation 0.04 Å) and parallel (see Fig. 2) and lie perpendicular to the crystallographic mirror planes, running along $2a - c$. Each ribbon has six near neighbours (see Fig. 2) and shows edge-to-edge interactions (CH···Cl 2.83 Å, Cl···Cl 3.520 Å) and face-to-face interactions of *ca.* 3.5 Å. Each $[\text{PtCl}_4]^{2-}$ lies directly beneath (and above) a pyridinium ring (Pt-centroid distance 3.472 Å). The Pt···Pt distance along the ribbon is 15.76 Å, while the shortest Pt···Pt distance is 6.665 Å. The bipyridine unit is planar (torsion angle at the central carbon–carbon bond = 1.0°). Similarly the $[\text{PtCl}_4]^{2-}$ and $[4,4'\text{-H}_2\text{bipy}]^{2+}$ ions are coplanar, leading to the pyridinium *ortho* hydrogens lying in the plane of the *cis*-PtCl_2 unit at CH···Cl distances 2.96 Å (*i.e.* just above the sum of the van der Waals radii, 2.95 Å) and Cl···H–C 114°, and Pt–Cl···HC 141°.

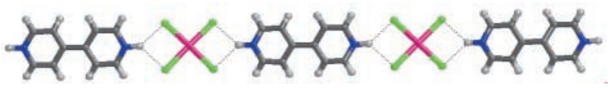

Fig. 1 Structure of one polymeric ribbon in crystalline $[4,4'\text{-H}_2\text{bipy}][\text{PtCl}_4]$ **2**. The NH···Cl hydrogen bonds are indicated.

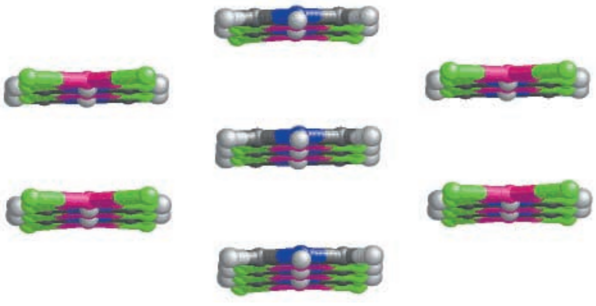

Fig. 2 The crystal structure of $[4,4'\text{-H}_2\text{bipy}][\text{PtCl}_4]$ **2** viewed along the ribbon shown in Fig. 1.

In contrast, the structure of $[4,4'\text{-H}_2\text{bipy}][\text{CoCl}_4]$ **3**, first reported by Atwood and co-workers[17] is markedly different from that in **2** with the tetrahedral $[\text{CoCl}_4]^{2-}$ units forming two-centre Cl···HN interactions in a dimeric cyclic $[4,4'\text{-H}_2\text{bipy}]_2[\text{CoCl}_4]_2$ motif of form **C** in which there are no interactions of type **A**, but rather each NH hydrogen bonds to just one M–Cl unit within the dimer unit and to no other chloride.

Table 1 Selected bond and hydrogen bond[a,b] lengths (Å) and angles (°) in crystals of [4,4′-H_2bipy][MCl_4] (**2**–**8**) and [4,4′-H_2bipy][MBr_4] (**10**–**12**)

Compound	**2** (Pt, Cl)	**3** (Co, Cl)	**4** (Zn, Cl)	**5** (Hg, Cl)	**6** (Mn, Cl)	**7** (Cd, Cl)	**8** (Pb, Cl)	**10** (Co, Br)	**11** (Zn, Br)	**12** (Mn, Br)
M–X terminal/Å	2.3019(14)	2.2626(13) 2.2683(13) 2.2959(14) 2.2960(13)	2.2526(7) 2.2546(7) 2.2934(7) 2.2977(8)	2.4382(13) 2.4681(13) 2.5050(14) 2.5187(13)	2.4904(6)	2.5733(8)	2.7538(12)	2.3883(8) 2.3960(8) 2.4239(8) 2.4289(8)	2.3885(7) 2.3934(7) 2.4285(7) 2.4320(7)	2.6454(6)
M–X bridging/Å					2.5946(7), 2.6294(6)	2.6673(8), 2.7031(7)	2.9452(14), 3.0044(12)			2.7498(6), 2.7562(4)
$MX_{term}\cdots HN$/Å	2.40	2.32, 2.63	2.30, 2.63	2.28, 2.74	2.51	2.54	2.56	2.46, 2.84	2.46, 2.85	2.67
$MX_{term}\cdots HC$/Å	2.83	2.58, 2.68, 2.68, 2.75, 2.77, 2.81, 2.85	2.56, 2.65, 2.67, 2.74, 2.75, 2.83, 2.83	2.60, 2.70, 2.70, 2.71, 2.77, 2.82, 2.86	2.77, 2.82	2.79, 2.81	2.75, 2.88, 2.89	2.73, 2.82, 2.83, 2.85, 2.88, 2.96, 2.96	2.72, 2.84, 2.85, 2.85, 2.89, 2.95, 2.96	2.93, 2.95
$MX_{bridge}\cdots HN$/Å					2.58	2.60	2.68			2.75
$MX_{bridge}\cdots HC$/Å					2.70, 2.85	2.72, 2.85	2.84			2.87, 2.99
cis-X–M–X/°	89.92(7), 90.08(7)				93.09(3), 87.84(2), 92.69(3), 96.15(2), 91.12(2), 92.95(2), 79.71(2)	93.65(4), 87.27(2), 92.91(3), 96.35(2), 91.41(2), 91.54(2), 80.62(2)	86.21(5), 88.78(4), 91.14(4), 95.29(4), 93.22(4), 86.87(4), 83.55(5)			92.73(3), 88.585(13), 91.07(3), 95.878(16), 91.056(15), 91.477(16), 81.462(16)
trans-X–M–X/°	180.0				170.83(2), 169.43(2)	172.03(2), 168.65(3)	179.89(4), 175.42(3)			172.500(11), 169.95(3)
Tetrahedral X–M–X/°		110.16(5), 107.03(5), 110.71(5), 106.19(5), 111.04(5), 111.53(5)	110.76(3), 110.61(3), 107.37(3), 111.00(3), 106.39(3), 110.58(3)	112.85(5), 114.86(5), 101.07(5), 112.43(4), 104.48(5), 110.14(5)				109.82(3), 105.97(3), 111.96(3), 107.30(3), 109.99(3), 111.62(3)	110.39(3), 106.45(2), 111.66(3), 107.37(3), 110.05(3), 110.76(3)	
M–X–M/°					100.29(2)	99.38(2)	93.13(4)			98.538(16)
$M–X_{term}\cdots HN$/°	92.4	115.6, 90.9	115.9, 90.6	112.0, 88.4	94	94	90	114, 89	114, 89	94
$MX_{term}\cdots H–N$/°	136	156, 140	156, 139	162, 136	134	134	133	157, 139	156, 138	135
$M–X_{term}\cdots HC$/°	126	124, 91, 109, 130, 90, 146, 98	124, 91, 109, 130, 91, 147, 98	121, 103, 124, 89, 88, 143, 96	115, 142	114, 141	91, 110, 157	125, 126, 105, 88, 92, 145, 100	125, 126, 105, 89, 90, 100, 146	114, 138
$M–X_{term}\cdots H–C$/°	131	151, 138, 176, 137, 133, 126, 125	151, 176, 138, 137, 133, 125, 125	145, 134, 142, 169, 129, 121, 123	132, 116	130, 117	136, 115, 126	148, 141, 134, 174, 133, 124, 125	150, 142, 134, 178, 135, 126, 126	129, 119
$M–X_{bridge}\cdots HN$/°					95, 90	95.4, 89.8	94, 90			96, 90
$MX_{bridge}\cdots H–N$/°					132	131	132			133
$M–X_{bridge}\cdots HC$/°					89, 138; 87, 116	88, 138; 86, 115	99, 136			89, 135; 86, 116
$MX_{bridge}\cdots H–C$/°					133, 116	131, 117	120			132, 118

[a] Only Cl···H contacts < 2.95 Å and Br···H contacts < 3.10 Å are quoted. [b] Values quoted for hydrogen bonds are based on hydrogen atom positions determined by X-ray diffraction.

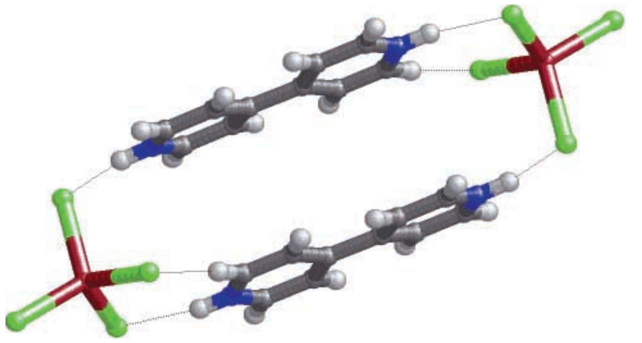

Fig. 3 Structure of the hydrogen bonded dimeric ring in [4,4′-H_2bipy][$ZnCl_4$] **4**. The NH · · · Cl CH · · · Cl hydrogen bonds are indicated.

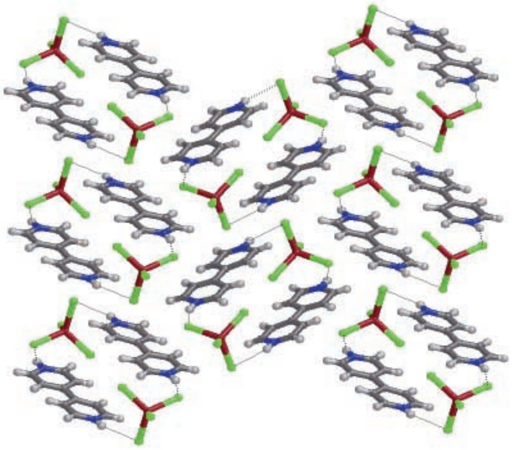

Fig. 4 The crystal structure of [4,4′-H_2bipy][$ZnCl_4$] **4**. The NH · · · Cl hydrogen bonds are indicated.

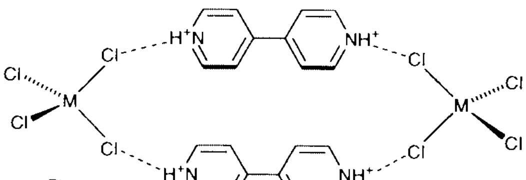

C

In the course of the attempted preparation of mixed metal salts of [4,4′-H_2bipy]$^{2+}$ (for which full details will be presented elsewhere) we isolated samples of **3** and recorded low temperature diffraction data for comparison with its zinc and mercury analogues **4** and **5**. In all these cases we obtained crystalline salts [4,4′-H_2bipy][MCl_4] [M = Co (**3**), Zn (**4**) and Hg (**5**)] by routes employing aqueous solutions containing M^{2+} and 4,4′-bipyridinium and chloride ions. The three phases are isostructural (see Figs. 3–5) and contain ions of normal dimensions having one short NH · · · Cl hydrogen bond of length *ca.* 2.30 Å and a second longer one of length 2.63–2.75 Å (see Table 1). The shorter NH · · · Cl hydrogen bond is itself part of a R2,2(7) interaction **D** involving a second chloride ligand and one of the *ortho*-CH groups (CH · · · Cl 2.65–2.71 Å). There are a further six CH · · · Cl interactions of length < 2.95 Å between the neutral cyclic {[4,4′-H_2bipy][MCl_4]}$_2$ units (2.56–2.86 Å, see Table 1). These interactions lead to a herring-bone-like packing of these dimer units (see Fig. 4) in which the bipy moieties are near planar (central torsion angle 5.7° in **3**, 6.7° in **4**, and 15.7° in **5**). An alternative reading of this structure is possible in which the coplanarity of the [4,4′-H_2bipy]$^{2+}$ ions and chloride ligands of the tetrachlorometallate ions is emphasised and leads to ruffled sheets containing chloride ligands and [4,4′-H_2bipy]$^{2+}$ ions cross-linked by the metals (see Fig. 5).

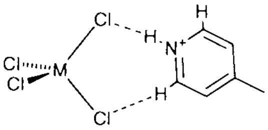

D

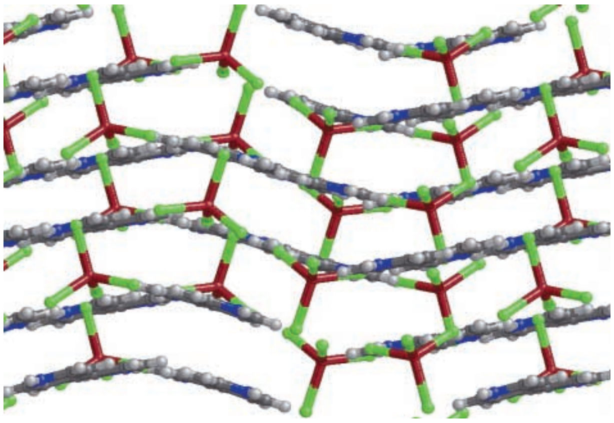

Fig. 5 The crystal structure of [4,4′-H_2bipy][$ZnCl_4$] **4** viewed approximately parallel to the ruffled sheets containing chloride ligands and [4,4′-H_2bipy] cations.

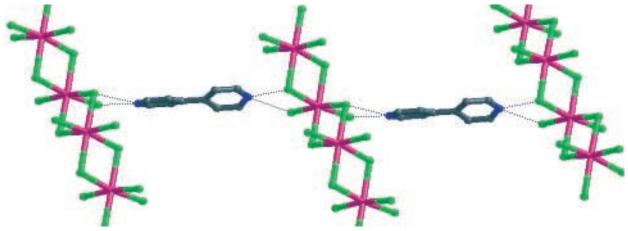

Fig. 6 Part of a layer formed by {[MCl_4]$^{2-}$}$_n$ chains cross-linked by hydrogen bonding to [4,4′-H_2bipy] in crystalline [4,4′-H_2bipy][MCl_4] [M = Mn (**6**), Cd (**7**)]. All hydrogens are omitted for clarity. The N · · · Cl hydrogen bonds are indicated.

When the analogous manganese compound [4,4′-H_2bipy][$MnCl_4$] **6** was prepared by the same route as **3**–**5**, in the expectation that it too would be isomorphous with **3** it was surprising to discover that it has a quite different structure (see Fig. 6). Salt **6** contains octahedral $MnCl_6$ units linked by *cis* edge-sharing into chains (**E**). The [{$MnCl_4$}$_n$]$^{2n-}$ chains are hydrogen bonded to [4,4′-H_2bipy]$^{2+}$ forming neutral sheets perpendicular to *b*. Interactions **A** are formed at both ends of the dication (see **F** and Fig. 6) and at both sides of the [{MCl_4}$_n$]$^{2n-}$ chain, as in **G**, so as to form ribbons **B** through the structure. The cross-linking of [{MCl_4}$_n$]$^{2n-}$ chains by the hydrogen bonded ribbon

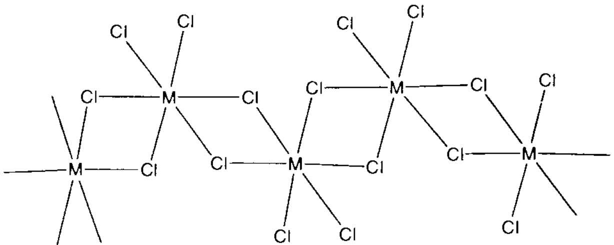

E

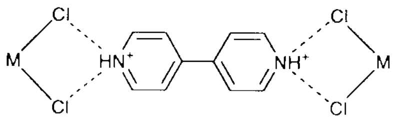

F

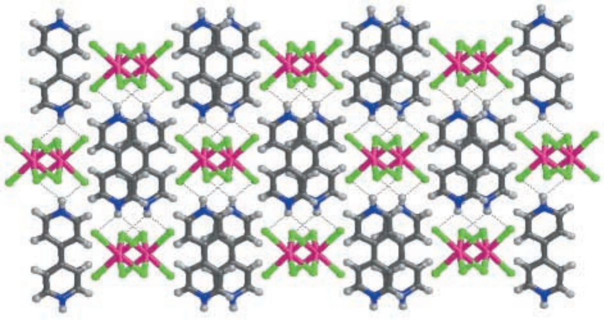

Fig. 7 The crystal structure of [4,4′-H$_2$bipy][MCl$_4$] [M = Mn (**6**), Cd (**7**)] viewed along the {[MCl$_4$]$^{2-}$}$_n$ chains and parallel to the layers of {[MCl$_4$]$^{2-}$}$_n$ chains cross-linked by hydrogen bonding to [4,4′-H$_2$bipy]$^{2+}$. The NH···Cl hydrogen bonds are indicated.

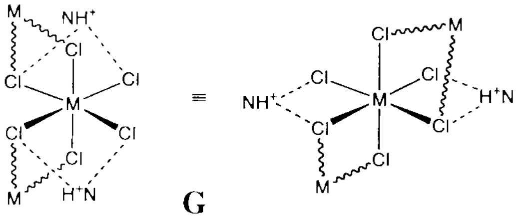

G

leads to neutral layers (see Fig. 7). The Mn···Mn distance within the **E** chain is 4.011 Å while the Mn···Mn distance along the **B**-type ribbons is 15.59 Å. The ribbons **B** extend along a+2c, while the [{MCl$_4$}$_n$]$^{2n-}$ chains **E** extend along c.

The many [MnCl$_4$]$^{2-}$ salts known show only two structure types: (a) tetrahedral [MnCl$_4$]$^{2-}$ and (b) a ⟨100⟩ layer perovskite structure with sheets of corner-sharing {MnCl$_6$} octahedra as in **H**.[10,18] Similar behaviour is seen for tetrahalide salts of Cd(II) in the Cambridge Structural Database (CSD).[14,19] In these layer perovskites the primary ammonium cations each make three strong NH···Cl hydrogen bonds per NH$_3$ group (see **I**), and this is held to be a key factor in stabilising the **H** layers. To test the generality of the formation of the new chain structure type in the presence of [4,4′-H$_2$bipy]$^{2+}$ we chose cadmium and lead chloride salts for study. Crystalline [4,4′-H$_2$bipy][CdCl$_4$] **7** is readily prepared and is isostructural with its manganese analogue. It shows two interactions **A** per dication (NH···Cl lengths 2.54 and 2.60 Å in **7** for the terminal and bridging chloride ligands, respectively; *cf.* 2.51, 2.58 in **6**) and two CH···Cl bonds per chlorine (see Table 1). The Cd···Cd distance within the **E** chain is 4.095 Å while the Cd···Cd distance along the **B**-type ribbons is 15.996 Å.

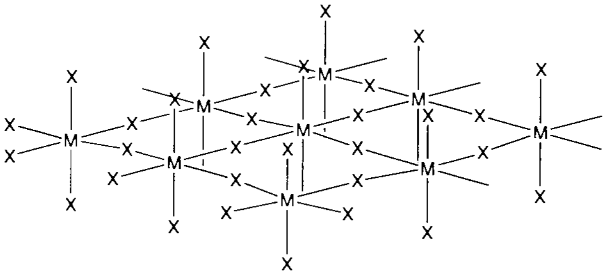

H

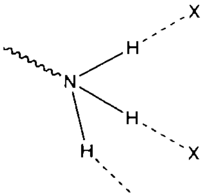

I

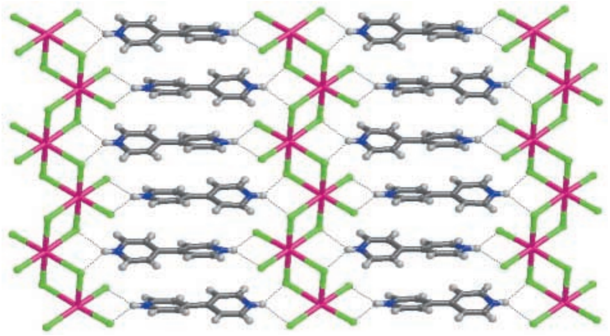

Fig. 8 A layer of the [4,4′-H$_2$bipy][PbCl$_4$] **8** crystal structure showing {[PdCl$_4$]$^{2-}$}$_n$ chains cross-linked by hydrogen bonding to [4,4′-H$_2$bipy]$^{2+}$.

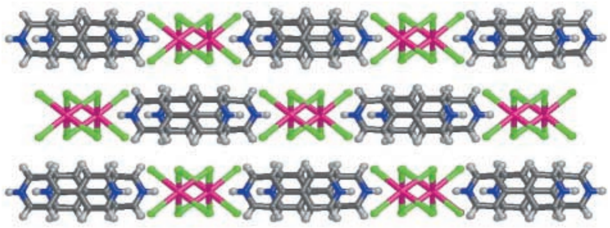

Fig. 9 The crystal structure of [4,4′-H$_2$bipy][PbCl$_4$] **8** viewed along the {[PbCl$_4$]$^{2-}$}$_n$ chains and parallel to the layers shown in Fig. 8.

The analogous lead(II) salt [4,4′-H$_2$bipy][PbCl$_4$] **8**, prepared in the same way, has a structure similar but not identical to that of **6** and **7** (see Table 1, Figs. 8 and 9). In **8** the same type **E** [{MCl$_4$}$_n$]$^{2n-}$ chains are present (Pb···Pb distance 4.321 Å) linked by synthon **A** and motif **B** (Pb···Pb distance along ribbon 16.458 Å = b) as in **6** and **7**. However, in **6** and **7** the *cis*-MCl$_2$···HN interaction, **A**, involves one terminal and one bridging chloride ligand from the **E** chain at each end of the [4,4′-H$_2$bipy]$^{2+}$ (see **G**). In **8** this interaction involves two terminal chlorides at one end and two bridging chlorides at the other end of the [4,4′-H$_2$bipy]$^{2+}$ cation (see Fig. 8 and **J**). The NH···Cl distances are 2.56 and 2.68 Å for the terminal and bridging chloride ligands respectively. The net result is formation of neutral layers (see Fig. 9) of stoichiometry [4,4′-H$_2$bipy][PbCl$_4$]. The layers in **8** form from a face of the [{MCl$_4$}$_n$]$^{2n-}$ chain orthogonal to that in salts **6** and **7**. In **8** the **B** ribbons extend along unit cell direction y, while the [{MCl$_4$}$_n$]$^{2n-}$ chains once again extend along c. There are three weak CH···Cl bonds per terminal chloride (2.75, 2.88 and 2.89 Å) and one per bridging chloride (2.84 Å). The bipy moieties in motif **B** of **6**–**8** are more twisted than in **2** or **3**–**5** (central torsion angle 20.7, 21.8 and 16.8° in **6**–**8**, respectively).

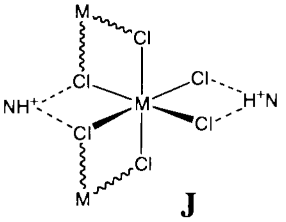

J

Use of similar synthetic procedures but replacing chloride with bromide led to preparation of a series of analogous bromide salts [4,4′-H$_2$bipy][MBr$_4$] [M = Pd (**9**), Co (**10**), Zn (**11**), Mn (**12**)]. The crystal structures of **10**–**12** were determined (see Tables 1 and 2) and together with powder diffraction measurements on **9**–**12** showed all four of these bromide species to be strictly isostructural with their chloride analogues. The bipy moieties show central torsion angles of 12.9° in **10**, 9.1° in **11** and 22.5° in **11**). In **12** the Mn · · · Mn distance within the **E** polymer chains is 4.172 Å, while the Mn · · · Mn distance in the **B**-type motif is 16.324 Å. The difference between M–Br bond lengths and the corresponding M–Cl distances in the analogous chloride salts averages 0.129, 0.136 and 0.146 Å for **10**, **11** and **12**, respectively. The mean difference between the EH · · · Br and corresponding EH · · · Cl hydrogen bond lengths is 0.18 Å for E = N and 0.15 Å for E = C.

Discussion

Based on the observation that metal chloride complexes are effective hydrogen bond acceptors,[12] we have shown that supramolecular synthons such as **A** may be exploited to prepare designed metal-containing hydrogen-bonded polymers of type **B** in $[4,4'\text{-}H_2bipy]^{2+}$ salts of perhalometallates. Compound **2**, $[4,4'\text{-}H_2bipy][PtCl_4]$, illustrates the concepts which form the basis of this work. The supramolecular *synthon* (**A**) is present in the one-dimensional periodic *motif* (**B**). We can identify the *frameworks* [*i.e.* the square planar Pt(II) centre and the 4,4′-biaryl moiety] which carry the required *synthon components* (*i.e.* *cis*-MCl_2 and NH^+). The molecular *building blocks* of the structure are the ions ($[4,4'\text{-}H_2bipy]^{2+}$ and $[PtCl_4]^{2-}$). The linear hydrogen bond network formed in this case results from the linear disposition of the synthon components on the frameworks of the building blocks.

Contemporaneously with our report of **1** and **2**,[13] Rivas and Brammer reported[20] the preparation of chloroplatinate salts of $[H_2dabco]^{2+}$ (dabco = 1,4-diazabicyclooctane). These included a kinked chain polymer in the $[PtCl_4]^{2-}$ salt which contained synthon **A** and the beautiful structure of the $[PtCl_6]^{2-}$ salt in which the ribbon polymer **B** is replaced by an analogous hydrogen bonded chain with nearly circular cross-section formed by the three-fold symmetric $[PtCl_6]^{2-}$ and $[H_2dabco]^{2+}$ ions in which the chains are hexagonally close-packed.

That synthon **A** may have general applicability is indicated by the similarity of the structures of **2** (and **1** and **9**) and those of $[4,4'\text{-}H_2bipy][Cu_2(\mu\text{-}X)_2X_4]$ (X = Cl, Br) which were prepared for rather different reasons.[21,22] In these structures hydrogen bonded ribbon motifs are also present with planar $[Cu_2(\mu\text{-}X)_2X_4]$ (X = Cl, Br) dianions replacing the $[PtCl_4]^{2-}$ units in **2**. Clearly both the synthon and motif are robust enough to allow change of both metal (*e.g.* Pd for Pt) and halides (*e.g.* Br for Cl).

There are three families of structures for $[4,4'\text{-}H_2bipy][MX_4]$ salts reported here. Motif **B** is present when the metal anion is square planar (M = Pt, Pd), or polymerised to form a chain of edge-sharing MX_6 octahedra of type **C** (M = Mn, Cd, Pb). In the latter structure, motifs **B** cross-link the $[\{MX_4\}_n]^{2n-}$ chains **E** to form neutral two-dimensional sheets. The third class of $[4,4'\text{-}H_2bipy][MX_4]$ structure, seen for tetrahedral metal ions (M = Zn, Co, Hg) has neutral moieties **C** close-packed in a herring-bone manner. Synthon **A** is not formed in these latter structures, presumably because the increased Cl–M–Cl angle implied by the tetrahedral coordination at the metal requires a much shorter M · · · HN distance, as well as smaller M–Cl · · · HN and larger N–H · · · Cl angles than those seen in cases such as **2**, **6**–**8** and **12** where the Cl–M–Cl angle is *ca.* 90°. The longer NH · · · Cl contact observed in the ring dimer shown in Fig. 3 is soft and subject to substantial distortion as is reflected in its extension to 2.75 Å in **5**, presumably in order to accommodate the larger $[HgCl_4]^{2-}$ anion. Despite this, or perhaps because of the flexibility of this aspect of the structure, the complex packing in **3**–**5**, **10** and **11** is robust enough to accommodate a wide variety of metallate anions.

The $\{MX_4\}_n$ substructure **E** seen in **6**–**8** (X = Cl) and **12** (X = Br) is present in the $ZrCl_4$ structure[23] and is a substructure of the $CdCl_2$ structure.[24] It seems that the $[4,4'\text{-}H_2bipy]^{2+}$ cation plays a key role in promoting the formation of the **E** chain but only in those cases where the anion will tolerate polymerisation and the associated expansion of the metal coordination number from four to six. The comparison of this new structure type with that of the ⟨100⟩ layer perovskite structure[10,18] and the anionic polymer layers **H** within it is instructive. The chain structures of **6**–**8** and **12** have four bridging and two terminal halides per metal as does **H**. However **H** has more nearly linear M–X–M bridges (*ca.* 160–165° *cf.* 100.29(2), 99.38(2), 93.13(4) and 98.538(16)° in **6**–**8** and **12**, respectively). The implication is that bridging halides are strained in **H**, and that the more numerous NH · · · Cl bonds (see **I**, six per metal, *cf.* two NH per metal in **6**–**8** and **12**) compensate. However, it is not merely the number of hydrogen bond donors per metal that controls MX_4 polymerisation. Thus $[Hpy]_2[MnCl_4]$[25] has tetrahedral anions. In the present study the $[4,4'\text{-}H_2bipy][MX_4]$ (M = Co, Zn, Hg) salts **3**–**5**, **10** and **11** contain tetrahedral rather than polymeric anions. Why? It seems clear that the ability of the metal to adopt octahedral coordination is another key factor. Among primary ammonium salts, the $[NH_3(CH_2)_nNH_3][MCl_4]$ (n = 2, 3) (M = Zn or Co) have tetrahedral dianions, while in other cases, *e.g.* M = Cr, Mn, Fe, Ni, Cd or Cu, structure **H** is adopted. All eight salts containing ions of empirical formula $[PbCl_4]^{2-}$ in the CSD have the layer perovskite structure **H**. The mercury case is interesting in that the mixed $[NH_3(CH_2)_2NH_3]_2[HgCl_4]Cl_2$ salt occurs in two forms, one a polymeric structure with five-coordinate mercury(II) centres,[26] and a second with a very distorted layer perovskite structure containing anions with four short Hg–Cl contacts (*i.e.* quasi-four-coordinate mercury),[27] while the analogous salt $[NH_3(CH_2)_3NH_3]_2[HgCl_4]Cl_2$ has the layer perovskite structure.[28] Of the other 30 structures in the CSD containing ions of empirical formula $[HgCl_4]^{2-}$, 28 have tetrahedral anions (albeit often rather distorted from T_d symmetry), one is trimeric and one is dimeric. Apparently mercury is able to form octahedral polymers but not as readily as, say manganese, cadmium or lead. It is notable that those metal ions most prone to form polymers by expansion of coordination from tetrahedral to octahedral are high spin d^5 (Mn) and d^{10} (Cd) or $d^{10}s^2$ (Pb). Finally we note that to date there is no example of the $NbCl_4$ structure type (linear chain *trans* edge-sharing octahedra) among the $[\{MCl_4\}_n]^{2n-}$ polymers identified to date.

It seems clear from these results that the $[4,4'\text{-}H_2bipy]^{2+}$ cation is instrumental in stabilising and perhaps in forming the unique edge-sharing octahedral chains in **6**–**8** and **12**. It has been known for many years that organo-cations (such as tetralkylammoniums) may play important roles in templating the hydrothermal formation of microporous solids such as zeolites. Furthermore there has been a spate of recent reports by Rao and others of the range of structures formed under the influence of hydrogen bonding primary ammonium cations in lower temperature syntheses of framework solids containing anionic ligands such as phosphate[29] and oxalate.[30] It may be that by appropriate choice of organic cation still more such solids with a wider range of architectures may be obtained. Clearly the pyridinium moiety offers a very different shape and hydrogen bond donor set to the anionic acceptors in such systems as compared with the $R_nNH_{4-n}{}^+$ set more often used.

While control of crystal structure by molecular structure and properties is at the heart of crystal engineering, the converse, control of molecular structure and properties by crystal structure, is also critical. The observation of the control of the cation over the form of the anion discussed above is the most striking example of this in this present work. In addition the cation used here is flexible by virtue of the torsion in the central C–C bond, as are some of the anions, and their structures are influenced by the crystal environment. As noted above the central twist in the $[4,4'\text{-}H_2bipy]^{2+}$ cation varies from near zero to over 20° in **2**–**8** and **10**–**12**, and is notably planar in the planar ribbons of **2**. The efficient packing that results presumably compensates for any unfavourable *ortho* · · · *ortho* H · · · H contacts that result within the cation. As noted by Brock and Minton such effects are common in biphenyl derivatives.[31] Similarly, the planarity of the anions in $[4,4'\text{-H}_2\text{bipy}][\text{Cu}_2(\mu\text{-Cl})_2\text{Cl}_4]$[21] is unusual. Of 25 other salts of $[\text{Cu}_2(\mu\text{-Cl})_2\text{Cl}_4]^{2-}$ in the CSD, 21 have non-planar geometry and near-tetrahedral geometry at Cu (with a dihedral angle between the $\text{Cu}_2(\mu\text{-Cl})_2$ and Cu_2Cl_4 planes of between 36 and 77°) and four have near-planar geometries (dihedral angle $< 8°$). In $[4,4'\text{-H}_2\text{bipy}][\text{Cu}_2(\mu\text{-Cl})_2\text{Cl}_4]$, as in **2**, efficient packing results from planarity in both cation and anion and is presumably decisive in forcing the less favoured molecular geometry.

The hierarchy of interactions present in these structures is interesting to consider. In complex salts such as these, the important intermolecular interactions contributing to the lattice energy might reasonably be expected to be as listed as below:

(1) Electrostatic (Madelung) interactions between the complex ions.
(2) Classical hydrogen bonding (of type D–H···A where D and A = O, N, S or halogen).
(3) Weak hydrogen bonding (of type D–H···A where D or A = C or other elements of low electronegativity).
(4) Dispersive (van der Waals) interactions.

The actual balance of these interactions is not clear and must await evaluation probably by computational methods. Clearly the emphasis placed on interactions of type (2) in this paper is a great simplification and there are both an abundance of type (3) interactions and potentially substantial electrostatic effects at work. Good shape match between the component ions in these salts must also be important. Synthon **A** requires short NH···Cl contacts but also implies that the *ortho*-CH hydrogens are close to the chloride ligands as in **K**. In practice these CH···Cl contacts appear to be at about the sum of the van der Waals radii implying that they do not contribute very much to the stabilisation of the structure. Equally they do not destabilise the structure seriously, and hence they imply a good shape fit between anion and cation in structures **1**, **2**, **6**–**9** and **12**. While shape fit (or complementarity) is less glamorous than potentially strongly attractive components of the lattice energy it is a prerequisite for such interactions.

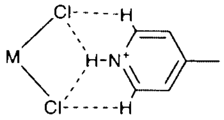

K

The related issue of the presence of groups that might interfere with the desired synthons (*e.g.* by themselves having hydrogen bonding capability) is also important here and in this kind of crystal engineering. The question is how robust is the synthon and or motif employed and how tolerant is it of other functional groups? Thus secondary hydrogen bond donor and acceptor sites (*e.g.* CH donors in pyridinium cations) or metal···halide interactions may interfere with, or be tolerated by, the primary synthons being used. It would seem in the cases reported here that the choice of anions without hydrogen bond donor sites and cations with strong hydrogen bond donors only within the synthon component is a successful strategy. However it is clear that interference is possible and indeed probable in other cases, from the solvent and or counter ions employed in the synthesis of the target solids. Thus the inclusion of water or chloride, tetraalkylammonium or other counter ions is not observed in the preparation of **1**–**12** but has been in other work on similar systems not reported here.[32]

The structures we have prepared to date are based on anionic perhalometallate hydrogen bond acceptors and cationic pyridinium N–H donors. This kind of salt system offers some key opportunities. Its modularity lends itself to exploration of a wide range of combinations of anions and cations (and solvents, counter ions and crystallisation methods), although as noted above there is the potential for deviation from the planned solids as a result of interference from solvent or counterions.

Given the success of our strategy to date, the construction of more complex and varied targets may be contemplated. The strategy may be summarised as "Synthon + Frameworks = Network" where the synthon is of type **A** say, the frameworks are the 4,4′-biaryl unit and the metal coordination sphere, and the network formed is a linear chain in motif **B**. Given reliable performance of the synthon, variation of the frameworks might provide a rational approach to preparation of networks of a variety of topologies determined by branching induced within the organic cation or the complex anion. Thus the slightly elaborated version of **A** shown in **L** might be used to link a range of different 4-pyridinium-substituted moieties. The frameworks used in this work have been covalent in the organic cation (and dative covalent in the anions) but there is no *a priori* reason not to use supramolecular frameworks when appropriate, and there may be reasons so to do in order to manipulate solubility or other properties of the target compounds. In the structures of **2**, **6**–**8** and **12** clear one- and two-dimensional substructures are evident. Use of cations with additional strong hydrogen bond donors may be helpful in adding additional dimension(s) to the hydrogen bond networks formed, given the presence of unused hydrogen bond acceptor capability on the anions. In this way ribbons might be cross-linked to form layers or layers to form three dimensional architectures.

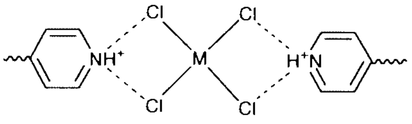

L

The unit cell dimensions in **6** (and the isostructural **7**), **8**, **12** (and in one respect **2**) are closely related as must be the case given the relationship between their structures. Similarly the unit cells in the isostructural set **3**–**5**, **10** and **11** are similar but not identical. Thus *c* in **6**–**8** and **12** is *ca.* 7 Å and corresponds to the M···M second-nearest neighbour distance along the type **E** chain in these structures. The M···M distance along the **B** ribbon in these structures is *ca.* 16 Å and corresponds to the unit cell *b* axis length in **8**, $a + 2c$ in **6**, **7** and **12** and $2a - c$ in **2**. The variation in these dimensions is small but significant (range *ca.* 7% in *c* within **6**–**8** and **12**, range of M···M distances of *ca.* 6% in motif **B**, and *ca.* 8% in motif **E**, and ranges of 2.2, 4.5 and 4.5% in *a*, *b* and *c*, respectively, within the set **3**–**5**, **9**, **10**). This metric variation raises the prospect of adjusting unit cell dimensions in a controlled manner by doping different amounts of a second metal (say Cd) into, for example, the manganese sites in **6** or doping the halide sites. Indeed if such isostructural mixed metal (or mixed halide) solids can be prepared they would offer not only the potential to control the metrics but also the prospect of manipulating the electronic, optical, magnetic or other properties of these crystalline materials.

The structures reported here incorporate reliable supramolecular synthons and motifs and offer the opportunity of more general methods of preparing diverse and controllable structures containing a wide variety of metals. Perhaps most importantly they show structural repetitivity, a concept central to the whole project of crystal structure synthesis.

Experimental

Syntheses and recrystallisations were carried out in air in standard glassware without special precautions except as noted below. Microanalyses were carried out by the staff of the

Microanalytical Service of the School of Chemistry, University of Bristol. The syntheses of **1**, **4**, **6**, and **7** and an alternative preparation of **2** have been reported previously.[13,14]

Syntheses of [4,4′-H_2bipy][MCl_4] [M = Pt (2), Co (3), Hg (5), Pb (8)] and [4,4′-H_2bipy][MBr_4] [M = Pd (9), Co (10), Zn (11), Mn (12)]

2. Addition of a yellow solution of $K_2[PtCl_4]$ (419 mg, 1.009 mmol) to a colourless solution of 4,4′-bipy (155 mg, 0.994 mmol) in HCl (5 cm^3, 33%) in H_2O (10 cm^3) caused the immediate formation of a orange microcrystalline insoluble precipitate of **2**. The product was washed with H_2O and dried *in vacuo*, yield 328 mg (66%). Microanalytical data (%). Found: C, 24.46; H, 1.38; N, 5.43. Calc.: C, 24.26; H, 2.04; N, 5.66. A sample of **2** for single crystal structure analysis was prepared using purpose designed "H-tube" glassware consisting of two parallel Schlenk tubes held vertically and joined by a horizontal tube with a vertical side arm. The tubes were partly filled with reagent (one with aqueous $K_2[PtCl_4]$ and the other with aqueous [4,4′-H_2bipy]Cl_2). Plugs of cotton wool were inserted into each tube and the apparatus filled with water to allow very slow diffusion of the reagent. Crystallisation occurred in the horizontal tube section over a period of weeks.

3. Addition of a pink solution of $CoCl_2$ (133 mg, 1.024 mmol) and $[Bu_4N]Cl$ (555 mg, 1.997 mmol) in H_2O (10 cm^3) and a colourless solution of $MnCl_2$ (157 mg, 1.091 mmol) and $[Bu_4N]Cl$ (560 mg, 2.015 mmol) in H_2O (10 cm^3) to a colourless solution of 4,4′-bipy (314 mg, 2.013 mmol) in HCl (5 cm^3, 33%) in H_2O (10 cm^3). Blue crystals were grown by slow cooling with simultaneous slow evaporation. Yield 173 mg (45%). Microanalytical data (%). Found: C, 33.79; H, 2.79; N, 7.27. Calc.: C, 33.45; H, 2.79; N, 7.81.

5. Addition of a colourless solution of 4,4′-bipy (158 mg, 1.013 mmol) in HCl (10 cm^3, 33%) to a colourless solution of $HgCl_2$ (272 mg, 1.002 mmol) in HCl (10 cm^3, 33%). Opaque crystals were grown by slow cooling with simultaneous slow evaporation. Yield 104 mg (21%). Microanalytical data (%). Found: C, 23.84; H, 1.89; N, 5.36. Calc.: C, 23.99; H, 2.01; N, 5.60.

8. Addition of a boiling colourless solution of 4,4′-bipy (314 mg, 2.013 mmol) in HCl (10 cm^3, 33%) to a boiling colourless solution of $PbCl_2$ (555 mg, 1.995 mmol) and $[Bu_4N]Cl$ (1.114 g, 4.013 mmol) in HCl (20 cm^3, 33%). Pale yellow crystals were grown by slow cooling of the reaction mixture. Yield 827 mg (82%). Microanalytical data (%). Found: C, 23.55; H, 1.90; N, 5.15. Calc.: C, 23.68; H, 1.99; N, 5.52.

9. Addition of a yellow solution of $K_2[PdBr_4]$ (1004 mg, 2 mmol) in H_2O (10 cm^3) to a colourless solution of 4,4′-bipy (312 mg, 2 mmol) in aqueous HBr (20 cm^3, 2.4%) caused the immediate formation of a red–brown microcrystalline insoluble precipitate of **9**. The product was washed with H_2O and dried *in vacuo*, yield 1092 mg (94%). Microanalytical data (%). Found: C, 20.02; H, 1.47; N, 4.04. Calc.: C, 20.55; H, 1.79; N, 4.79.

10. Addition of a pink solution of $CoBr_2$ (328 mg, 1.5 mmol) and KBr (358 mg, 3 mmol) in H_2O (10 cm^3) to a colourless solution of 4,4′-bipy (234 mg, 1.5 mmol) in aqueous HBr (20 cm^3, 2.4%). The pink solution was heated to reduce its volume. Green crystals were grown by slow cooling with simultaneous slow evaporation. Yield 725 mg (90%). Microanalytical data (%). Found: C, 22.73; H, 1.81; N, 5.13. Calc.: C, 22.36; H, 1.86; N, 5.22.

11. Addition of a solution of $ZnBr_2$ (348 mg, 1.5 mmol) and KBr (358 mg, 3 mmol) in H_2O (10 cm^3) to a colourless solution of 4,4′-bipy (234 mg, 1.5 mmol) in aqueous HBr (20 cm^3,

Table 2 Crystal and refinement data for [4,4′-H_2bipy][MCl_4] (**2**–**8**) and [4,4′-H_2bipy)][MBr_4] (**10**–**12**). All X-ray data were collected at 173 K

Compound	**2** (Pt, Cl)[a]	**3** (Co, Cl)[b]	**4** (Zn, Cl)	**5** (Hg, Cl)	**6** (Mn, Cl)	**7** (Cd, Cl)	**8** (Pb, Cl)	**10** (Co, Br)	**11** (Zn, Br)	**12** (Mn, Br)
Formula	$C_{10}H_{10}Cl_4N_2Pt$	$C_{10}H_{10}Cl_4N_2Co$	$C_{10}H_{10}Cl_4N_2Zn$	$C_{10}H_{10}Cl_4N_2Hg$	$C_{10}H_{10}Cl_4N_2Mn$	$C_{10}H_{10}Cl_4N_2Cd$	$C_{10}H_{10}Cl_4N_2Pb$	$C_{10}H_{10}Br_4N_2Co$	$C_{10}H_{10}Br_4N_2Zn$	$C_{10}H_{10}Br_4N_2Mn$
Formula weight	495.09	358.9	365.37	500.59	354.94	412.40	507.64	536.77	543.21	532.78
Crystal system	Monoclinic	Monoclinic	Monoclinic	Monoclinic	Monoclinic	Monoclinic	Monoclinic	Monoclinic	Monoclinic	Monoclinic
Space group (no.)	$I2/m$ (no. 12)	$P2_1/c$ (no. 14)	$P2_1/c$ (no. 14)	$P2_1/c$ (no. 14)	$C2/c$ (no. 15)	$C2/c$ (no. 15)	$C2/c$ (no. 15)	$P2_1/c$ (no. 14)	$P2_1/c$ (no. 14)	$C2/c$ (no. 15)
a/Å	6.6548(14)	7.6754(25)	7.6507(12)	7.7629(12)	15.526(2)	15.612(3)	13.012(3)	7.8207(9)	7.8031(8)	15.9959(18)
b/Å	11.695(2)	19.7420(65)	19.765(4)	20.2701(34)	12.660(3)	12.746(2)	16.458(3)	20.621(2)	20.594(2)	13.1476(15)
c/Å	8.146(3) Å	9.4908(32)	9.5012(18)	9.3418(15)	6.914(2)	7.0261(12)	7.3920(11)	9.692(11)	9.7596(9)	7.1305(8)
β/°	91.320(3)	108.992(6)	108.826(15)	107.414(13)	114.90(2)	114.984(3)	119.997(12)	107.804(2)	107.916(2)	114.992(2)
V/Å^3	633.9(3)	1359.8(8)	1359.9(4)	1402.6(4)	1232.6(5)	1267.3(4)	1370.9(4)	1488.2(3)	1492.3(3)	1359.2(3)
Z	2	4	4	4	4	4	4	4	4	4
μ/mm^{-1}	11.89	2.02	2.542	11.71	1.912	2.542	13.22	11.872	12.335	12.708
Reflections collected	2029	14447	8553	9076	3826	6367	4404	7896	9661	4384
Unique data	765	3126	3112	3207	1389	1448	1568	3391	3433	1575
R_{int}	0.065	0.1369	0.0327	0.0407	0.0189	0.0509	0.0445	0.0431	0.0443	0.0307
Final R_1 [$I > 2\sigma(I)$]	0.029	0.046	0.026	0.028	0.020	0.025	0.028	0.0364	0.0322	0.0268

[a] See ref. 13 for a less precise determination. [b] See ref. 17 for a room temperature determination.

2.4%). The pale yellow solution was stirred and left to evaporate slowly yielding large very pale yellow crystals. Yield 735 mg (90%). Microanalytical data (%). Found: C, 21.85; H, 1.75; N, 4.92. Calc.: C, 22.11; H, 1.84; N, 5.16.

12. Addition of a solution of $MnBr_2$ (440 mg, 2 mmol) and KBr (476 mg, 2 mmol) in H_2O (10 cm^3) to a colourless solution of 4,4′-bipy (312 mg, 2 mmol) in aqueous HBr (20 cm^3, 2.4%). The pale yellow solution was stirred and left to evaporate slowly yielding red–orange crystals. Yield 884 mg (83%). Microanalytical data (%). Found: C, 22.53; H, 1.74; N, 4.69. Calc.: C, 22.53; H, 1.88; N, 5.26.

Crystal structure analyses of [4,4′-H_2bipy][MCl_4] (2–8) and [4,4′-H_2bipy][MBr_4] (10–12)

Many of the details of the structure analyses of **2**–**8** and **10**–**12** are presented in Table 2. In each case a full hemisphere of reciprocal space was scanned with the area detector centre held at $2\theta = -27°$.

CCDC reference number 186/2114.

See http://www.rsc.org/suppdata/dt/b0/b005036i/ for crystallographic files in .cif format.

In **2** the metal atoms and cations lies at sites of C_{2h} symmetry. In **6**–**8** and **12** the metal atoms and the cations lie at sites of C_2 symmetry. All hydrogen atoms were located in difference maps. In **8** a second low occupancy [1.34(9)%] position for the lead atom was identified resulting from disorder.

X-Ray powder diffraction experiments on bulk samples of **2**–**8** and **10**–**12** were consistent with the presence of pure phases with the structures noted above. The powder patterns for **1** and **9** are consistent with both being strictly isostructural with **2**.

Magnetic measurements

The cryogenic magnetic susceptibility of microcrystalline [4,4′-H_2bipy]][$MnCl_4$] **6** was measured between room temperature and 2 K and shows an antiferromagnetic exchange coupling.[14]

Acknowledgements

Financial support of the Royal Society (a Royal Society China Royal Fellowship to X-M. W.) and from the Spanish Dirección General de Enseñanza Superior e Investigación Científica through Project PB97-1479-C02-02 is gratefully acknowledged.

References

1 G. R. Desiraju, *Angew Chem.*, *Int. Ed. Engl.*, 1995, **34**, 2311; G. R. Desiraju, *Chem. Commun.*, 1997, 1475.
2 J. C. MacDonald and G. M. Whitesides, *Chem. Rev.*, 1995, **28**, 37; F. H. Allen, P. R. Raithby, G. P. Shields and R. Taylor, *Chem. Commun.*, 1998, 1043; C. B. Aakeröy and K. R. Seddon, *Chem. Soc. Rev.*, 1993, **22**, 397; I. G. Dance, in *The Crystal as a Supramolecular Entity*, ed. G. R. Desiraju, *Perspectives in Supramolecular Chemistry*, Wiley, Chichester, vol. 2, 1996.
3 R. Robson, B. F. Abrahams, S. R. Batten, R. W. Gable, B. F. Hoskins and J. P. Liu, *ACS Symp. Ser.*, 1992, **499**, 256; S. R. Batten and R. Robson, *Angew. Chem.*, *Int. Ed.*, 1998, **37**, 1461; M. J. Zaworotko, *Chem. Soc. Rev.*, 1994, **23**, 283; L. Carlucci, G. Ciani, P. Macchi, D. M. Proserpio and S. Rizzato, *Chem. Eur. J.*, 1999, **5**, 237; L. Tei, V. Lippolis, A. J. Blake, P. A. Cooke and M. Schröder, *Chem. Commun.*, 1998, 2633; T. Iwamoto, S. Nishikiori, T. Kitazawa and H. Yuge, *J. Chem. Soc.*, *Dalton Trans.*, 1997, 4127.
4 J. C. M. Rivas and L. Brammer, *Coord. Chem. Rev.*, 1999, **183**, 43.
5 D. Braga, F. Grepioni and A. G. Orpen, *Organometallics*, 1994, **13**, 3544; D. Braga, F. Grepioni, E. Tedesco and A. G. Orpen, *J. Chem. Soc.*, *Dalton Trans.*, 1995, 1215.
6 N. G. Connelly, J. G. Crossley, A. G. Orpen and H. Salter, *J. Chem. Soc.*, *Chem. Commun.*, 1992, 1564; N. G. Connelly, J. G. Crossley and A. G. Orpen, *J. Chem. Soc.*, *Chem. Commun.*, 1992, 1568; D. A. Bardwell, J. G. Crossley, J. C. Jeffery, A. G. Orpen, E. Psillakis, E. E. M. Tilley, M. D. Ward, *Polyhedron*, 1994, **13**, 2291; N. G. Connelly, J. G. Crossley, A. G. Orpen and H. Salter, *J. Organomet. Chem.*, 1994, **480**, C12; H. Bois, J. G. Crossley, J. C. Guillorit, N. G. Connelly, G. R. Lewis, A. G. Orpen and P. Thornton, *J. Chem. Soc.*, *Dalton Trans.*, 1998, 2833.
7 T. B. Marder, N. C. Norman, A. G. Orpen, M. J. Quayle, C. R. Rice, *J. Chem. Soc.*, *Dalton Trans.*, 1999, 2127.
8 J. Starbuck, N. C. Norman and A. G. Orpen, *New J. Chem.*, 1999, **23**, 969.
9 S. C. James, N. C. Norman, A. G. Orpen and J. Starbuck, *Cryst. Eng. Commun.*, 2000, 10.
10 D. B. Mitzi, *Prog. Inorg. Chem.*, 1999, **48**, 1.
11 D. Braga, O. Benedi, L. Maini and F. Grepioni, *J. Chem. Soc.*, *Dalton Trans.*, 1999, 2611; C. B. Aakeroy A. M. Beatty and D. S. Leinen, *Angew. Chem.*, *Int. Ed.*, 1999, **38**, 1815; J. C. M. Rivas and L. Brammer, *New J. Chem.*, 1999, **22**, 1315; S. Ulvenlund, A. S. Georgopoulou, D. M. P. Mingos, I. Baxter, S. E. Lawrence, A. J. P. White and D. J. Williams, *J. Chem. Soc.*, *Dalton Trans.*, 1998, 1869.
12 G. Aullón, D. Bellamy, L. Brammer, E. A. Bruton and A. G. Orpen, *Chem. Commun.*, 1998, 653.
13 G. R. Lewis and A. G. Orpen, *Chem. Commun.*, 1998, 1873.
14 A. L. Gillon, A. G. Orpen, J. Starbuck, X.-M. Wang, Y. Rodríguez-Martín and C. Ruiz-Pérez, *Chem. Commun.*, 1999, 2287.
15 (*a*) G. P. A. Yap, A. L. Rheingold, P. Das and R. H. Crabtree, *Inorg. Chem.*, 1995, **34**, 3474; (*b*) P. J. Davies, N. Veldman, D. M. Grove, A. L. Spek, B. T. G. Lutz and G. van Koten, *Angew. Chem.*, *Int. Ed. Engl.*, 1996, **35**, 1959.
16 G. A. Jeffery, *Introduction to Hydrogen Bonding*, Wiley, Chichester, 1997; G. A. Jeffery and W. Saenger, *Hydrogen Bonding in Biology and Chemistry*, Springer Verlag, Berlin, 1993.
17 L. J. Barbour, L. R. MacGillivray and J. L. Atwood, *Supramol. Chem.*, 1996, **7**, 167.
18 P. Day, *J. Chem. Soc.*, *Dalton Trans.*, 1997, 701.
19 F. H. Allen, J. E. Davies, J. J. Galloy, O. Johnson, O. Kennard, C. F. Macrae, E. M. Mitchell, G. F. Mitchell, J. M. Smith and D. G. Watson, *J. Chem. Inf. Comput. Sci.*, 1987, **31**, 187; F. H. Allen and O. Kennard, *Chem. Des. Automat. News*, 1993, **8**, 1; F. H. Allen and O. Kennard, *Chem. Des. Automat. News.*, 1993, **8**, 31.
20 J. C. M. Rivas and L. Brammer, *Inorg. Chem.*, 1998, **37**, 4756.
21 M. Bukowska-Strzyzewska and A. Tosik, *Pol. J. Chem.*, 1979, **53**, 2423.
22 A. Tosik, M. Bukowska-Strzyzewska and J. Mrozinski, *J. Coord. Chem.*, 1990, **21**, 253.
23 B. Krebs, *Z. Anorg. Allg. Chem.*, 1970, **378**, 263.
24 L. Pauling and J. L. Hoard, *Z. Kristallogr. A*, 1930, **74**, 546.
25 C. Brassy, R. Robert, B. Bachet and R. Chevalier, *Acta Crystallogr.*, *Sect. B*, 1976, **32**, 1371.
26 Huo Wen, S. E. Miller, D. A. House, V. McKee and W. T. Robinson, *Inorg. Chim. Acta*, 1992, **193**, 77.
27 R. Spengler, R. Zouari, A. Ben Salah, H. Zimmermann and H. Burzlaff, *Acta Crystallogr.*, *Sect. C*, 1998, **54**, IUC 9800034.
28 R. Spengler, R. Zouari, H. Zimmermann, A. Ben Salah and H. Burzlaff, *Acta Crystallogr.*, *Sect. C*, 1998, **54**, 1628.
29 See, for example: C. N. R. Rao, S. Natarajan and S. Neeraj, *J. Am. Chem. Soc.*, 2000, **122**, 2810.
30 R. Vaidhyanathan, S. Natarajan, A. K. Cheetham and C. N. R. Rao, *Chem. Mater.*, 1999, **11**, 3636.
31 C. P. Brock and R. P. Minton, *J. Am. Chem. Soc.*, 1989, **111**, 4586.
32 A. Angeloni, A. L. Gillon, A. G. Orpen and S. A. Rotter, unpublished work.